

Seismic behaviour of arch dams including site effects

V.D. Milovanovitch

Ecole Nationale des Ponts et Chaussées, Paris, France

P. Thomas

Electricité de France, DER, Clamart, France

E. Bourdarot

Electricité de France, CNEH, Le Bourget du Lac, France

ABSTRACT: The seismic response of an arch dam to nonuniform ground motions is studied to assess the importance of spatial variation of earthquake angle of incidence as well as of fluid-structure interaction (effects of water compressibility) in that conditions. The method uses the multiple-support seismic excitation based on the three-dimensional earthquake wave representation with a given number of "shape functions". Depending on surface topography this method uses the harmonic P, SV, SH and Rayleigh waves developed in Taylor series as well as the more complex earthquake signal representation. The three-dimensional analysis shows the most inconvenient directions of angle of incidence for different wave types and the considerable importance of water compressibility effects for lower wave celerities. Also, the shape of "possible earthquake" that gives the maximum damage at the chosen part of the dam (or the whole dam) is determined, depending on the number of "shape functions".

1 INTRODUCTION

The finite earthquake wave celerity can have significant importance to the seismic response of large structures when the earthquake wave takes a finite travel time across the structure foundations. Also, the rock nature (discontinuous, anisotropic and non-homogeneous medium) brings modifications in signal frequencies and amplitudes between an earthquake source and a site. The irregular (non-plane) surface topography, with its canyon and mountains (or reservoir cavities only), particularly in the structure vicinity, can have the significant influence on dynamic characteristics of the site and on seismic behaviour of the structure.

Some recent studies, analysing the arch dam response (in linear domain) to nonuniform canyon motions, used only several angles of incidence, estimated them like the most important and treated the upstream-downstream direction perpendicular to the cross-stream direction. The aim of the study presented here, is to make the general solution for the spatial variation of angle of incidence on the nonsymmetric dam-water-foundation system.

2 METHOD USED

In the case of an arch dam, the presence of great water volume leads us to take into account the dam-water interaction, for which the water compressibility is considered. Since the good quality rock site is one of necessary conditions to construct an arch dam, the arch dam-foundation interaction effects have certain importance but not so great as it could be in the case of soil-structure interaction. For the purposes of this study the adequate dam-water-foundation system is used.

The method uses the multiple-support seismic excitation based on the three-dimensional earthquake wave representation with a given number of "shape-

functions" [1]. The time history as well as the frequency analyses with appropriate "shape-functions" can be performed. Each "shape-function" represents the surface of any form that defines the distribution of the imposed displacements on the finite element mesh boundary. In the time domain, the excitation represents the sum of the corresponding "shape-function"-acceleration (speed and displacement) products.

In the frequency domain, if the surface topography changes are not important against model dimensions, the harmonic P, SV, SH and Rayleigh waves are developed in Taylor series and each of them represents the sum of the "shape-functions" (geometric functions) multiplied by the different complex coefficients depending on angle of incidence, angle of direction, wave length, material properties, excitation frequency and amplitude. This variable separation allows the 3D angle of incidence and angle of direction sweeping [1]. The economic effect lies in the fact that the number of computations of the FE model is limited to the number of "shape-functions" that can be very important in the case of large models. The divergences of P, SV, SH and Rayleigh wave approximations depend on the number of terms in Taylor series and they vary in space depending on angle of incidence and on angle of direction. Adopted damage criterion represents the integral of elastic energy of deformation (the sum of the distortion and volume change energies) over the defined frequency range. The excitation is imposed on the FE mesh boundary as the movements (in the rock depth) obtained by using the superposition of the incident and reflected waves treating the domain as semi-infinite without structure and without canyon. In 3D angle of incidence and angle of direction sweeping, with the arbitrary canyon form, the scattering wave problem becomes very complicated.

If the surface topography changes are important against model dimensions, the seismic signal is not treated as a wave but as a more complex movements.

Using the Rayleigh quotient and keeping the same "shape-functions", their coefficients are determined to obtain the maximum damage in the structure, normalized with regard to the earthquake energy of the smallest "cube" containing the model. Therefore, the shape of the "possible earthquake", that gives the maximum damage at the chosen point of the structure, can be determined [1]. The comparison between the maximum damages for different number of "shape functions", at the same point of the structure, gives the function with asymptotic property which means that the maximum damage is limited and it does not increase after a certain number of "shape-functions".

The dam-water interaction method is based on the symmetric mixed variational formulation [4] extended to the multiple-support excitation domain. The earthquake analysis uses the mode superposition method with nonproportional damping (coupled modal co-ordinate equations of motion). The mode analysis frequency range (defined by the cut-off frequency) has to be sufficiently larger than the seismic analysis frequency range. The contribution of the modes with frequencies higher than the cut-off frequency is replaced by the pseudomode (the static correction).

For the purposes of this study the FE computer program EXCITM [2] was made, using CRAY Y-MP hardware.

3 MODELS CONSIDERED

As an example, a dam-water-foundation system considered is the FE model of recently constructed double curvature arch dam of Electricité de France (the Laparan arch-dam, 106 m height, 280 m crest length). The dam and the near field rock (200 m in depth) surrounding the whole reservoir with the dam are discretized with volume solid elements. The whole reservoir (1000 m long, 550 m large) is discretized with volume fluid elements. The solid-fluid contact surface is discretized with surface coupling elements. This model has 6716 nodes and 6776 elements. For an eigenproblem, that makes the system with 15000 DOF and 7.5 million terms in symmetric system matrix while for a seismic analysis that makes the system with 18500 DOF and 10.5 million terms in symmetric system matrix. The material properties used for the dam concrete are: dynamic elasticity modulus 60000 MPa, Poisson's ratio 0.20, specific density 2.45 kNs²/m⁴. The initial near field rock properties are: dynamic elasticity modulus 56000 MPa (corresponds to P wave celerity of 5000 m/s or S wave celerity of 2900 m/s), Poisson's ratio 0.25, specific density 2.70 kNs²/m⁴.

This study includes 12 considered FE models used for analysis of influence of different parameters.

The FE mesh used in the reservoir was rather dense (3177 fluid elements) to allow a good accuracy of acoustic eigenmodes.

4 EIGENVALUE ANALYSES

The cut-off frequency for all eigenvalue analyses was 10 Hz. In most of the models the first 60 eigenmodes were determined using the base of 120 vectors (Lanczos method). To clearly distinguish different types of

eigenmodes in the solid-fluid coupling problem with compressible water, the modal energies are computed (potential and kinetic energies of solid and fluid as well as their coupling energy). In all eigenvalue analyses the first mode was antisymmetric and the first three modes were dam modes with different added masses of water. The first acoustic mode of the model with rigid foundations was at 5.25 Hz (the 14th mode), of the model with deformable foundations ($E_r=56000$ MPa) was at 5.83 Hz (4th mode) and of twice shorter model with deformable foundations was at 6.31 Hz (12th mode). The modal pressures in the reservoir show the volume of "active" water in each eigenmode. In the case of incompressible water there are neither acoustic nor coupling eigenmodes. All of them are of the same type: solid mode with the added mass of water. The presence of deformable foundations and the water compressibility gives the important increase in eigenfrequency density.

The free surface condition was pressure equal to zero. It means that the sloshing modes are neglected because there are hundreds of sloshing modes with frequencies in the same range as the lower system frequencies. The shifting technique can not help much.

5 SEISMIC ANALYSES

The seismic analyses were made in the range of frequency from 0 to 5 Hz. In the far field rock the four different mediums were used, defined by P wave celerities: $c_{pf}=5000$ m/s, $c_{pf}=10000$ m/s, $c_{pf}=20000$ m/s and $c_{pf}=\text{infinite}$ celerity (uniform excitation). The ratio between P wave and S wave celerity was approximately 1.73 and between Rayleigh wave and S wave was 0.92. In the near field rock two different mediums were used, whose P wave celerities were: $c_{pn}=5000$ m/s and $c_{pn}=\text{infinite}$ celerity. The specific energy was calculated at 24 dam points (12 on upstream and 12 on downstream face) chosen as typical.

The damping coefficients used for the dam were 5% and 10% for the first and the last mode in the mode analysis frequency range. The corresponding damping coefficients for the near field rock were 10% and 20% and for the water they were nearly zero.

The three-dimensional angle of incidence ($0^\circ \leq \theta \leq 90^\circ$ - measured from vertical axis) and angle of direction ($0^\circ \leq \varphi \leq 360^\circ$ - measured from positive dam axis) sweepings are performed using the angle step of 5° .

The angle between the approximate reservoir direction and the dam axis is about 25° in the case of longer reservoir (1000 m length) and about 40° in the case of shorter reservoir (500 m length).

The 12 FE models used, allow the analysis of influence of different parameters: angle of incidence, angle of direction, wave type, celerity of wave propagation in the far field and near field rock, comparison between compressible and incompressible water effects, comparison between full and empty reservoir, model and reservoir shapes, model and reservoir dimensions.

6 SOME RESULTS AND CONCLUSIONS

1. Using the surfaces presented on the figures 1 and 3 as examples, the maximum energy depending on angle of incidence θ and angle of direction φ can be

determined, for different types of waves (P, SV, SH and Rayleigh waves) at any point of the dam. These angles θ and φ determine the most inconvenient wave directions for the given dam. After this type of analysis the dam designer can perform the seismic analysis of the dam with these dangerous directions.

For the dam sites for which exist the intervals of dominating angles θ and φ , these analyses are important for the choice of the dam site, dam position and than the final study of dam response.

2. The dam response to SV waves is much more important than the response to three other wave types together. In the case of $c_{pf} = 5000$ m/s and compressible water, the total energy in the abutment zone due to SV waves is 14, 15 and 5.5 times greater than energies due to P, SH and Rayleigh waves respectively.

3. When the wave propagation celerity in the far field rock increases, the total energy in the dam decreases for all types of waves. The energy in the abutment zone has the largest decrease between $c_{pf} = 5000$ m/s and $c_{pf} = 10000$ m/s. On the other hand, there is no significant difference in energy between $c_{pf} = 20000$ m/s and $c_{pf} = \infty$ celerity.

4. The most important amount of energy in dam is due to SV waves, then follow Rayleigh waves, P and SH waves.

5. When the rock is softer the energy in dam increases.

6. For SV waves, the ratio between dam energies for compressible and incompressible water, in the case of $c_{pf} = 5000$ m/s, is about 2 to 3. When the celerity in the far field rock increases this ratio decreases: for $c_{pf} = 10000$ m/s the ratio is about 1.4 to 1.5 and for $c_{pf} = 20000$ m/s is about 1.0 to 1.1. For P waves, in the case of $c_{pf} = 5000$ m/s the same ratio is about 1.4 to 1.5. For SH waves, this ratio is about 0.95 to 0.6 but the dam energies are negligible comparing with energies due to SV waves. For Rayleigh waves, this ratio is about 5 to 10 for different celerities and different locations in the dam.

7. It is evident that the water compressibility has important effects on the dam response especially for lower wave celerities (softer rock) and it is necessary to take it into account.

8. The reservoir influence is dominant comparing with influence of small changes of model shape and near field rock mass distribution.

9. In the case of $c_{pf} = 5000$ m/s, the increasing of reservoir length twice (from 500 m to 1000 m) increases the energy in dam for all wave types.

For $c_{pf} = 10000$ m/s, P waves give approximately the same dam energy regardless of this reservoir length change. SV waves provide much more energy in the dam, in the case of long reservoir. SH waves provide some more energy for the long reservoir than for the short one.

In the case of $c_{pf} = 20000$ m/s, P waves provide some more energy for the short reservoir comparing with the long one. SV and SH waves provide some more energy for the long reservoir. Rayleigh waves have greater influence for the long reservoir than in the case of SV waves.

In the case of infinite celerity, P waves provide the same energy for the long and short reservoir. SV waves provide also the same energy for both cases.

10. The pseudostatic energies in the abutment zone are greater than anywhere else in the dam but they are all negligible in comparison with dynamic energies.

11. For P waves, the energy at the chosen dam point has always only one maximum value for all angles of incidence and angles of direction. For SV, SH and Rayleigh waves this energy can have several maximum values.

12. In the case of large models the economic advantage of this method lies in the fact that the number of computations of the FE model is limited to the number of "shape functions" and it does not depend on the angle step of θ and φ sweeping.

13. For each particular case it is recommended to perform the sweepings of angle of incidence θ and angle of direction φ and to determine the most inconvenient angles for different wave types.

14. As an example, for $c_{pm} = 5$ km/s and with compressible water, the most inconvenient angles of SV waves, for $c_{pf} = 5$ km/s, $c_{pf} = 10$ km/s, $c_{pf} = 20$ km/s and $c_{pf} = \infty$, are respectively: $\varphi = 25^\circ$, $\theta = 70^\circ$; $\varphi = 25^\circ$, $\theta = 70^\circ$; $\varphi = 15^\circ$, $\theta = 35.3^\circ$ (critical angle); $\varphi = 5^\circ$, $\theta = 35.3^\circ$ (critical angle). For incompressible water these angles of SV waves are respectively: $\varphi = 25^\circ$, $\theta = 35.3^\circ$; $\varphi = 15^\circ$, $\theta = 35.3^\circ$; $\varphi = 10^\circ$, $\theta = 35.3^\circ$; $\varphi = 0^\circ$, $\theta = 0^\circ$. For the empty reservoir these angles of SV waves are respectively: $\varphi = 25^\circ - 50^\circ$, $\theta = 35.3^\circ$; $\varphi = 25^\circ - 40^\circ$, $\theta = 35.3^\circ$; $\varphi = 20^\circ - 70^\circ$, $\theta = 35.3^\circ$; $\varphi = \text{dispersed}$, $\theta = 35.3^\circ$.

For $c_{pm} = 5$ km/s and with compressible water, the most inconvenient angles of P waves, for $c_{pf} = 5$ km/s, $c_{pf} = 10$ km/s, $c_{pf} = 20$ km/s and $c_{pf} = \infty$, are respectively: $\varphi = 205^\circ$, $\theta = 65^\circ$; $\varphi = 30^\circ - 80^\circ$ and $130^\circ - 160^\circ$, $\theta = 10^\circ$; $\varphi = 25^\circ$, $\theta = 15^\circ$; $\varphi = 185^\circ$, $\theta = 25^\circ$. For incompressible water these angles of P waves are respectively: $\varphi = 205^\circ$, $\theta = 70^\circ$; $\varphi = 15^\circ$, $\theta = 70^\circ$; $\varphi = 175^\circ$, $\theta = 70^\circ$; $\varphi = 185^\circ$, $\theta = 60^\circ$. For the empty reservoir these angles of P waves are respectively: $\varphi = 210^\circ$, $\theta = 70^\circ$; $\varphi = 25^\circ - 50^\circ$, $\theta = 70^\circ$; $\varphi = 10^\circ - 70^\circ$, $\theta = 65^\circ$; $\varphi = \text{dispersed}$, $\theta = 60^\circ$.

For $c_{pm} = 5$ km/s and with compressible water, the most inconvenient angles of SH waves, for $c_{pf} = 5$ km/s, $c_{pf} = 10$ km/s, $c_{pf} = 20$ km/s and $c_{pf} = \infty$, are respectively: $\varphi = 60^\circ$, $\theta = 90^\circ$; $\varphi = 65^\circ$, $\theta = 90^\circ$; $\varphi = 85^\circ$, $\theta = 90^\circ$; $\varphi = 95^\circ - 100^\circ$, $\theta = 0^\circ$. For incompressible water these angles of SH waves are respectively: $\varphi = 60^\circ$ and 350° , $\theta = 90^\circ$; $\varphi = 65^\circ$, $\theta = 90^\circ$; $\varphi = 80^\circ$, $\theta = 90^\circ$; $\varphi = 90^\circ$, $\theta = 0^\circ$. For the empty reservoir these angles of SH waves are respectively: $\varphi = 340^\circ$, $\theta = 90^\circ$; $\varphi = 340^\circ$, $\theta = 90^\circ$; $\varphi = 40^\circ - 65^\circ$, $\theta = 90^\circ$; $\varphi = \text{dispersed}$, $\theta = 0^\circ$.

For $c_{pm} = 5$ km/s and with compressible water, the most inconvenient angles of Rayleigh waves, for $c_{pf} = 5$ km/s, $c_{pf} = 10$ km/s, $c_{pf} = 20$ km/s and $c_{pf} = \infty$, are respectively: $\varphi = 15^\circ$; $\varphi = 25^\circ$; $\varphi = 25^\circ$; $\varphi = 190^\circ - 200^\circ$. For incompressible water these angles of Rayleigh waves are respectively: $\varphi = 205^\circ$; $\varphi = 25^\circ$; $\varphi = 20^\circ$; $\varphi = 185^\circ$. For the empty reservoir these angles of Rayleigh waves are respectively: $\varphi = 205^\circ$; $\varphi = 30^\circ$; $\varphi = 60^\circ - 70^\circ$; $\varphi = \text{dispersed}$.

15. The comparisons, at the corresponding dam points, between maximum damages for different number of "shape functions" show that the maximum damage is limited and it does not increase after a certain number of "shape functions".

16. Using the three basic "shape functions" (uniform excitations) the maximum dam energy is obtained for $\varphi = 180^\circ$, $\theta = 70^\circ$ in the case of incompressible water and for $\varphi = 180^\circ$, $\theta = 0^\circ - 45^\circ$ (for different dam points) in the case of compressible water.

Space limitations do not allow the presentation of all interesting results obtained in this study.

ACKNOWLEDGEMENTS

The authors are grateful to *Electricité de France, Centre National d'Équipement Hydraulique* and *Direction des Etudes et Recherches* for their financial support and for use of high performance Computer Center.

REFERENCES

- Milovanovitch, V. 1992. *Comportement dynamique des barrages en béton et prise en compte des effets de site sur les ondes sismiques incidentes*. Ph.D. Thesis. Ecole Nationale des Ponts et Chaussées. Paris.
- Milovanovitch, V. 1991. EXCITM - A computer program for 3D multiple-support earthquake analysis of concrete dams. *Electricité de France/DER. Report no. HP-61/91.165*. Clamart.
- Milovanovitch, V. & Thomas, P. 1991. Une méthode de calcul de la reponse sismique des structures étendues. *Workshop AFPS-AFPC "Ponts en zone sismique"*: 78-87. Saint-Rémy-lès-Chevreuse.
- Morand, H. & Ohayon, R. 1979. Substructure variational analysis of the vibrations of coupled fluid-structure systems. Finite element results. *Int.J.num. Meth.Engng.*,14,:741-755.

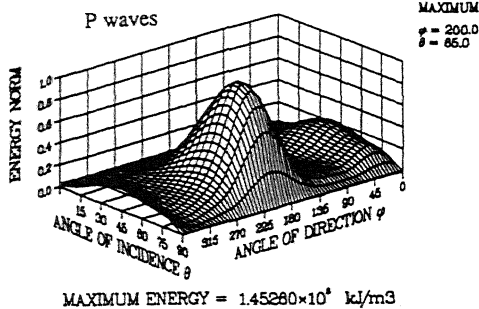


Figure 1-a. Total energy of deformation at the middle node of the dam crest on the upstream face, in function of angle of incidence θ and angle of direction ϕ . The celerity of P waves is 5000 m/s in the near field and far field rock. The water is compressible.

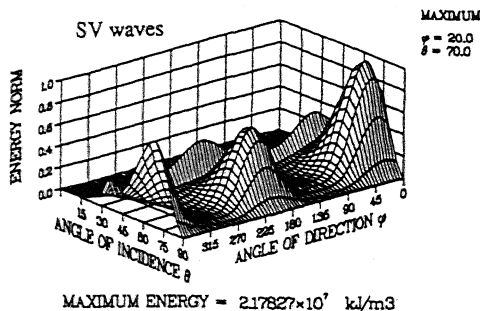


Figure 1-b. Total energy of deformation at the middle node of the dam crest on the upstream face, in function of angle of incidence θ and angle of direction ϕ . The celerity of SV waves is 2900 m/s in the near field and far field rock. The water is compressible.

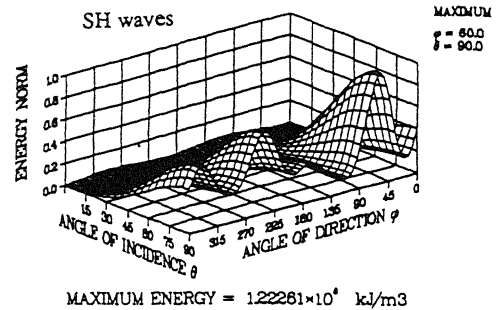


Figure 1-c. Total energy of deformation at the middle node of the dam crest on the upstream face, in function of angle of incidence θ and angle of direction ϕ . The celerity of SH waves is 2900 m/s in the near field and far field rock. The water is compressible.

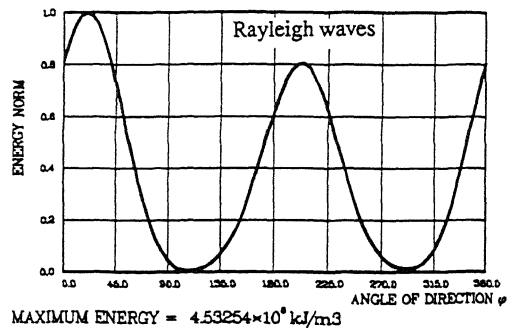


Figure 1-d. Total energy of deformation at the middle node of the dam crest on the upstream face, in function of angle of direction ϕ . The celerity of Rayleigh waves is 2650 m/s in the near field and far field rock. The water is compressible.

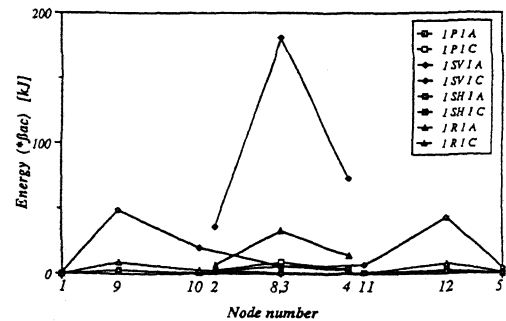
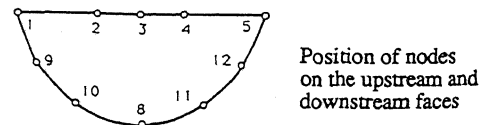


Figure 2-a. Influence of different wave types. The total energy in different dam node zones (A - nodes in the abutment zone; C - nodes in the crest zone). The celerities in the far field and near field rock are: 5000 m/s for P waves, 2900 m/s for S waves and 2650 m/s for Rayleigh waves. The water is compressible.

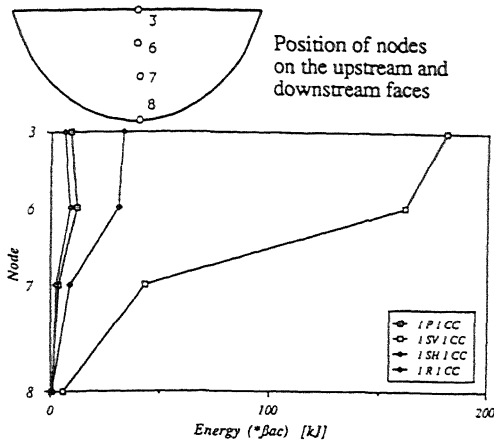


Figure 2-b. Influence of different wave types. The total energy in the central cantilever node zones. The celerities in the far field and near field rock are: 5000 m/s for P waves, 2900 m/s for S waves and 2650 m/s for Rayleigh waves. The water is compressible.

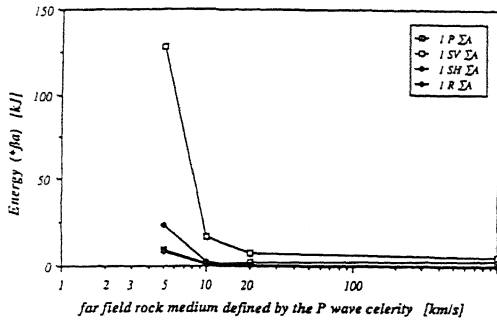


Figure 2-c. Influence of different wave types. The sum of total energies in the abutment zone as a function of P wave celerity in the far field rock. The P wave celerity in the near field rock is $c_{pn}=5000$ m/s. The water is compressible.

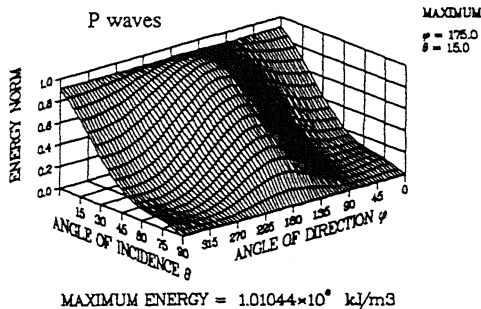


Figure 3-a. Total energy of deformation at the middle node of the dam crest on the upstream face, in function of angle of incidence θ and angle of direction ϕ . The celerity of P waves is 5000 m/s in the near field rock and 20000 m/s in the far field rock. The water is compressible.

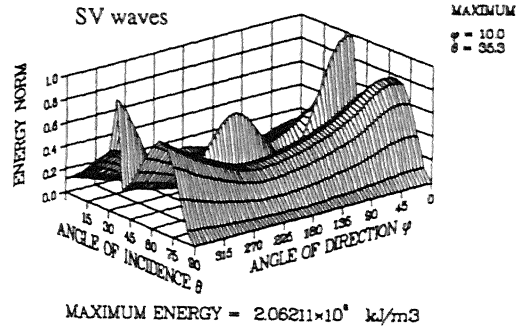


Figure 3-b. Total energy of deformation at the middle node of the dam crest on the upstream face, in function of angle of incidence θ and angle of direction ϕ . The celerity of SV waves is 2900 m/s in the near field rock and 11600 m/s in the far field rock. The water is compressible.

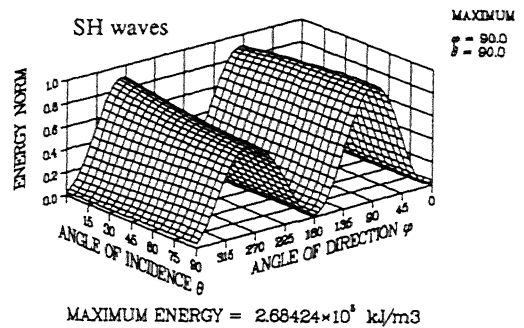


Figure 3-c. Total energy of deformation at the middle node of the dam crest on the upstream face, in function of angle of incidence θ and angle of direction ϕ . The celerity of SH waves is 2900 m/s in the near field rock and 11600 m/s in the far field rock. The water is compressible.

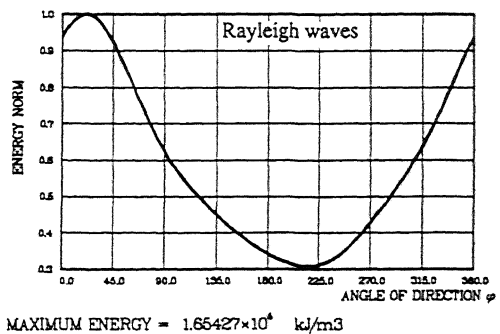


Figure 3-d. Total energy of deformation at the middle node of the dam crest on the upstream face, in function of angle of direction ϕ . The celerity of Rayleigh waves is 2650 m/s in the near field rock and 10600 m/s in the far field rock. The water is compressible.